



Mitigation of Transient Doppler Artifacts In Airborne Pulse Doppler Radar

Steven J. Hughes
Defence Research Establishment Ottawa

DEFENCE RESEARCH ESTABLISHMENT OTTAWA

TECHNICAL REPORT
DREO TR 1999-125
December 1999



Canada

DISTRIBUTION STATEMENT A
Approved for Public Release
Distribution Unlimited

DMC QUALITY INSPECTED

20000131 030



Mitigation of Transient Doppler Artifacts In Airborne Pulse Doppler Radar

Steven J. Hughes
*Pulse Doppler Radar Group
Aerospace Radar and Navigation Section*

DEFENCE RESEARCH ESTABLISHMENT OTTAWA

TECHNICAL REPORT
DREO TR 1999-125
December 1999

Project
3DE21

ABSTRACT

The Defence Research Establishment Ottawa has developed a Digital Radar Receiver and Data Acquisition System as part of an experimental air-to-air surveillance radar that will be used to demonstrate an air-to-air surveillance capability for the Canadian Forces CP-140 Maritime Patrol Aircraft. This report presents an analysis of the radar return signal expected from a point target, and predicts the existence of transient Doppler artifacts associated with the leading and trailing edges of the radar pulses. A software simulation also produces transient Doppler artifacts, and experimental measurements of a simulated target signal confirm their existence. The magnitude of the artifact is significant when a wideband receiver is used, that is, when the system bandwidth is not small with respect to the radar intermediate frequency. The potential impact of the artifacts on radar performance is discussed, as are techniques to mitigate their deleterious effects.

RÉSUMÉ

Le Centre de recherches pour la défense Ottawa a mis au point un récepteur radar numérique et un système d'acquisition de données faisant partie d'un radar de surveillance air-air expérimental qui sera utilisé pour doter l'avion de patrouille maritime CP-140 des Forces canadiennes de la capacité de surveillance air-air. Le rapport renferme une analyse de l'écho radar auquel on s'attend à partir d'une cible ponctuelle et prédit l'existence d'artefacts Doppler transitoires associés aux flancs avant et arrière des impulsions radar. De plus, une simulation informatisée produit des artefacts Doppler transitoires, et des mesures expérimentales d'un signal de cible simulé confirment leur existence. Le rapport étudie l'impact potentiel des artefacts sur les performances du radar ainsi que des techniques d'atténuation de leurs effets nuisibles.

EXECUTIVE SUMMARY

The role of the Canadian Forces CP-140 Maritime Patrol Aircraft is evolving to include new activities such as air-to-air surveillance in support of drug interdiction and other civil and military missions. To support these new roles, the Defence Research Establishment Ottawa has developed an experimental pulse-Doppler radar to demonstrate an air-to-air surveillance capability for the CP-140. This capability will permit the detection and tracking of small, slow, low-flying aircraft.

The report presents an analysis of the pulse Doppler return signal expected from a point target. The analysis predicts the existence of transient Doppler artifacts associated with the leading and trailing edges of the radar pulses. The maximum power level of the artifacts, relative to the maximum power level of the target signal, is shown to be inversely proportional to the square of the radar intermediate frequency. For the experimental air-to-air radar, the analysis predicts an artifact power level about 30 dB less than the target signal level, with the artifact occurring at a frequency that is the negative of the target signal Doppler frequency.

A software simulation of the quadrature demodulation of the pulse Doppler return signal from a point target produces a time-frequency image that exhibits transient Doppler artifacts similar to those predicted by the analysis. The maximum power level of the simulation artifact is about 27 dB less than the simulation target level. The simulation artifact appears in the time-frequency image at a frequency that is the negative of the target Doppler frequency.

Range-Doppler maps derived from experimental measurements of a synthetic target signal applied to the Digital Radar Receiver exhibit transient Doppler artifacts consistent with both the analysis and the software simulation. The maximum power level of the experimentally measured artifact is about 25 dB less than the synthetic target level. The experimentally measured artifact appears in the Range-Doppler map at a frequency that is the negative of the synthetic target Doppler frequency.

An air-to-air surveillance radar on the CP-140 would normally operate in a down-looking configuration, in which case the dominant noise source would be the return signal from the portion of the earth's surface illuminated by the main lobe of the antenna, that is, the main lobe clutter. The main lobe clutter will appear in a Range-Doppler map at a Doppler frequency determined by the aircraft speed and by the antenna look direction. The transient Doppler artifact associated with the main lobe clutter could potentially mask targets and reduce the detection performance of the radar.

Techniques are discussed to reduce the deleterious effects of the transient Doppler artifacts on the detection performance of the radar. These techniques include:

- using a Variable Frequency Oscillator to tune the Doppler frequency of the main lobe clutter, and its artifact, to zero;
- using pulses with non-zero rise and fall times to reduce the relative power level of the artifacts; and
- increasing the radar intermediate frequency to further reduce the relative power level of the artifacts.

Combining these techniques, the power level of the transient Doppler artifacts could be reduced to the noise floor of the radar receiver, at which point they would have little or no impact on system performance.

SOMMAIRE

Le rôle de l'avion de patrouille maritime CP-140 des Forces canadiennes évolue et comprend de nouvelles activités telles que la surveillance air-air à l'appui de la répression du trafic des drogues et d'autres missions civiles et militaires. Pour appuyer ces nouveaux rôles, le Centre de recherches pour la défense Ottawa a mis au point un radar à impulsions Doppler expérimental pour doter le CP-140 de la capacité de surveillance air-air. Cette capacité permettra la détection et la poursuite de petits aéronefs volant à basse altitude.

Le rapport renferme une analyse de l'écho d'impulsion Doppler auquel on s'attend à partir d'une cible ponctuelle. L'analyse prédit l'existence d'artefacts Doppler transitoires associés aux flancs avant et arrière des impulsions radar. Il est démontré que le niveau de puissance maximal des artefacts, par rapport au niveau de puissance maximal du signal de cible, est inversement proportionnel au carré de la fréquence intermédiaire du radar. Pour le radar air-air expérimental, l'analyse prédit un niveau de puissance d'artefact d'environ 30 dB inférieur à celui de la cible, l'artefact se produisant à une fréquence égale à la fréquence Doppler du signal de cible mais de signe négatif.

Une simulation informatisée de la démodulation en quadrature de l'écho d'impulsion Doppler venant d'une cible ponctuelle produit une image du temps fréquence qui présente des artefacts Doppler transitoires semblables à ceux prédis par l'analyse. Le niveau de puissance maximal de l'artefact de simulation est d'environ 27 dB inférieur à celui de la cible de simulation. L'artefact de simulation apparaît dans l'image du temps fréquence à une fréquence égale à la fréquence Doppler de la cible mais de signe négatif.

Des cartes de portée Doppler dérivées de mesures expérimentales d'un signal de cible synthétique appliquée au récepteur radar numérique présentent des artefacts Doppler transitoires compatibles avec l'analyse et la simulation informatisée. Le niveau de puissance maximal de l'artefact mesuré lors de l'expérience est d'environ 25 dB inférieur à celui de la cible synthétique. L'artefact mesuré lors de l'expérience apparaît dans la carte de portée Doppler à une fréquence égale à la fréquence Doppler de la cible synthétique mais de signe négatif.

L'antenne d'un radar de surveillance air-air à bord du CP-140 serait normalement orientée vers le bas, auquel cas la source de bruit prédominante serait l'écho venant de la partie de la surface de la Terre illuminée par le lobe principal de l'antenne, c'est-à-dire le clutter de lobe principal. Le clutter de lobe principal apparaît sur une carte de portée Doppler à une fréquence Doppler déterminée par la vitesse de l'aéronef et par l'orientation de l'antenne. L'artefact Doppler transitoire associé au clutter de lobe principal risque de masquer des cibles et de réduire les performances de détection du radar.

Le rapport étudie des techniques pour réduire les effets des artefacts Doppler transitoires nuisibles aux performances de détection du radar. Ces techniques comprennent :

- l'utilisation d'un oscillateur à fréquence variable pour accorder la fréquence Doppler du clutter de lobe principal, et de son artefact, à zéro;
- l'utilisation d'impulsions avec des temps de montée et de descente inégales à zéro afin de réduire le niveau de puissance relatif des artefacts;
- l'augmentation de la fréquence intermédiaire du radar en vue de réduire encore le niveau de puissance relatif des artefacts.

En combinant ces techniques, on pourrait réduire le niveau de puissance des artefacts Doppler transitoires jusqu'au plancher de bruit du récepteur radar, où leur impact sur les performances du système serait minime ou nul.

Hughes, Steven J., Atténuation des artefacts doppler transitoires dans le radar à impulsions doppler aéroporté. Le Centre de recherches pour la défense Ottawa, DREO TR 1999-125. décembre 1999. (en anglais)

CONTENTS

ABSTRACT.....	iii
RÉSUMÉ	iii
EXECUTIVE SUMMARY	v
SOMMAIRE	vi
LIST OF FIGURES.....	ix
1.0 INTRODUCTION	1
2.0 MATHEMATICAL ANALYSIS.....	2
2.1 PULSE DOPPLER RADAR SIGNAL	2
2.2 QUADRATURE DEMODULATION	3
2.3 TRANSIENT DOPPLER ARTIFACTS.....	6
3.0 SIMULATION RESULTS.....	8
4.0 EXPERIMENTAL RESULTS.....	10
4.1 HARDWARE DESCRIPTION	10
4.2 MEASUREMENTS	10
5.0 IMPACT ON RADAR PERFORMANCE	11
5.1 OPERATIONAL IMPACT	11
5.2 MITIGATION OF EFFECT.....	13
5.2.1 <i>Variable Frequency Oscillator</i>	13
5.2.2 <i>Pulse Shape</i>	17
5.2.3 <i>Increased Intermediate Frequency</i>	17
6.0 SUMMARY AND CONCLUSIONS	18
APPENDIX A. MATLAB PROGRAMS.....	20
REFERENCES	27

LIST OF FIGURES

Figure 2-1 Schematic diagram of a two-pole lowpass filter used to isolate the I&Q components of the baseband radar signal.....	3
Figure 2-2 Relative power of the positive Doppler term (target) and the negative Doppler term (artifact) for a 640 nanosecond pulse.....	6
Figure 2-3 Relative power of the positive Doppler term (target) and the negative Doppler term (artifact) for a 2 microsecond pulse.....	7
Figure 3-1 Time-Frequency image produced by the software simulation.....	9
Figure 3-2 Cross-sections in time through the simulated target and the artifact for the software simulation.....	9
Figure 4-1 Block diagram of the Digital Radar Receiver hardware.....	10
Figure 4-2 Range-Doppler map computed from the output of the Digital Radar Receiver due to application of the synthetic target signal.....	11
Figure 5-1 Range- Doppler map of simulated main lobe clutter generated by the <i>SAFIRE</i> radar simulation program.....	12
Figure 5-2 Range-Doppler map of simulated main lobe clutter with the addition of approximated transient Doppler artifacts.....	13
Figure 5-3 Range-Doppler map showing simulated main lobe clutter, thermal noise, and a target at a range of 48.2 kilometers.....	14
Figure 5-4 Cross sections in Doppler frequency (upper plot) and range gate (lower plot) through the target in Figure 5-3.....	14
Figure 5-5 Range-Doppler map showing the simulated main lobe clutter, thermal noise, and a target, with approximated transient Doppler artifacts (VFO off).....	15
Figure 5-6 Cross sections in Doppler frequency (upper plot) and range gate (lower plot) through the target in Figure 5-5 (VFO Off).....	15
Figure 5-7 Range-Doppler map showing the simulated main lobe clutter, thermal noise, and a target, with approximated transient Doppler artifacts (VFO on).....	16
Figure 5-8 Cross sections in Doppler frequency (upper plot) and range gate (lower plot) through the target in Figure 5-7 (VFO on).....	16
Figure 5-9 Time-Frequency image showing reduced transient Doppler artifacts for pulses with 80 nanosecond rise and fall times.....	17

1.0 INTRODUCTION

The role of the CP-140 Maritime Patrol Aircraft is expected to evolve to include new activities such as air-to-air surveillance in support of drug interdiction and other civil and military missions. However, the AN/APS-506 radar on the CP-140 was designed for submarine and ship detection, and is unsuitable for use in the air-to-air surveillance role. To help address this deficiency, the Defence Research Establishment Ottawa has developed an experimental pulse-Doppler radar to demonstrate an air-to-air surveillance capability for the CP-140 radar. This capability will provide the ability to detect and track small, slow, low-flying aircraft.

This report addresses the phenomenon of transient Doppler artifacts that can potentially degrade the detection performance of a radar system by masking otherwise detectable targets, and presents techniques that can be used to mitigate the deleterious effects of the artifacts.

Section 2.0 presents a mathematical analysis of the pulse Doppler return signal expected from a point target. The analysis predicts the existence of transient Doppler artifacts associated with the leading and trailing edges of the radar pulses. The maximum power level of the artifacts, relative to the maximum power level of the target signal, is shown to be inversely proportional to the square of the radar intermediate frequency. For the experimental air-to-air radar, the analysis predicts an artifact power level about 30 dB less than the target signal level, with the artifact occurring at a frequency that is the negative of the target signal Doppler frequency.

Section 3.0 presents a software simulation of the quadrature demodulation of the pulse Doppler return signal from a point target. The simulation produces a time-frequency image that exhibits transient Doppler artifacts similar to those predicted by the mathematical analysis in Section 2.0. The maximum power level of the simulation artifact is about 27 dB less than the simulation target level. The simulation artifact appears in the time-frequency image at a frequency that is the negative of the target Doppler frequency.

Section 4.0 presents a Range-Doppler map derived from experimental measurements of a synthetic target signal applied to the Digital Radar Receiver. The Range-Doppler map exhibits transient Doppler artifacts consistent with both the mathematical analysis in Section 2.0 and the software simulation in Section 3.0. The maximum power level of the experimentally measured artifact is about 25 dB less than the synthetic target level. The experimentally measured artifact appears in the Range-Doppler map at a frequency that is the negative of the synthetic target Doppler frequency.

Section 5.0 presents a discussion of the potential impact of the transient Doppler artifacts on the detection performance of a radar system, and considers techniques to mitigate the deleterious effects of the artifacts. The techniques considered include using a Variable Frequency Oscillator, using pulses with non-zero rise and fall times, and increasing the radar intermediate frequency. Combining these techniques, the power level of the transient Doppler artifacts could be reduced to the noise floor of the radar receiver, at which they would have little or no impact on system performance.

2.0 MATHEMATICAL ANALYSIS

This section presents a mathematical analysis of the quadrature demodulation of a pulse Doppler radar signal. In particular, the analysis is focused on the transient Doppler artifacts that are shown to exist after the leading and trailing edges of the radar pulses. The maximum power level of the artifacts, relative to the maximum power level of the target signal, is shown to be inversely proportional to the square of the radar intermediate frequency.

2.1 PULSE DOPPLER RADAR SIGNAL

The pulse Doppler radar return from a point target can be represented by a pulsed sinusoidal signal, offset in frequency from the radar intermediate frequency by the Doppler frequency of the target. The sinusoidal signal is given by

$$x_0(t) = \sin(\omega t) \quad (1)$$

where $\omega = 2\pi(f_0 + f_D)$ is the angular signal frequency (radians per second),
 f_0 is the radar intermediate frequency (Hz),
 f_D is the target Doppler frequency (Hz), and
 t is the time (seconds).

The n^{th} pulse in a sequence of N pulses can be described by

$$x_n(t) = [u(t - (n-1)T) - u(t - ((n-1)T + \tau))] x_0(t) \quad (2)$$

where n is the pulse number (1 to N),
 T is the pulse period, or pulse repetition interval (PRI),
 τ is the pulse width ($\tau \ll T$), and
 $u(t)$ is the unit step function defined by

$$u(t) = \begin{cases} 0, & t < 0 \\ 1, & t \geq 0 \end{cases} \quad (3)$$

For the experimental air-to-air radar, the pulse width is about 640 nanoseconds. The pulse period varies from 50 microseconds up to about 150 microseconds, corresponding to pulse repetition frequencies from 20 kHz down to about 6.6 kHz.

Each group of N pulses constitutes a coherent processing interval. The coherent processing interval is the time period over which the radar signal can be coherently integrated. In general, longer integration times improve signal to noise ratio and enhance the probability of detecting the targets. For the experimental air-to-air radar, each coherent processing interval is made up of 256 pulses. The pulse Doppler signal for one coherent processing interval is simply the sum of N of the pulses given in Equation 2:

$$x(t) = \sum_{n=1}^N x_n(t), \quad 0 \leq t < nT \quad (4)$$

2.2 QUADRATURE DEMODULATION

The quadrature demodulation process reduces the carrier frequency of the radar signal to zero by multiplying the signal given in Equation 4 by the complex exponential of the radar intermediate frequency [1]:

$$y(t) = x(t) e^{-i\omega_0 t} \quad (5)$$

where $\omega_0 = 2\pi f_0$ is the angular radar intermediate frequency (radians per second).

Let the signal represented by $y(t)$ in Equation 5 be applied as a complex voltage to the input of the two-pole lowpass filter shown schematically in Figure 2-1. The complex output voltage, $z(t)$, represents the In-phase and Quadrature-phase (I&Q) components of the baseband radar signal. The remainder of this section is devoted to deriving a mathematical expression for $z(t)$, when $y(t)$ is given by Equation 5.

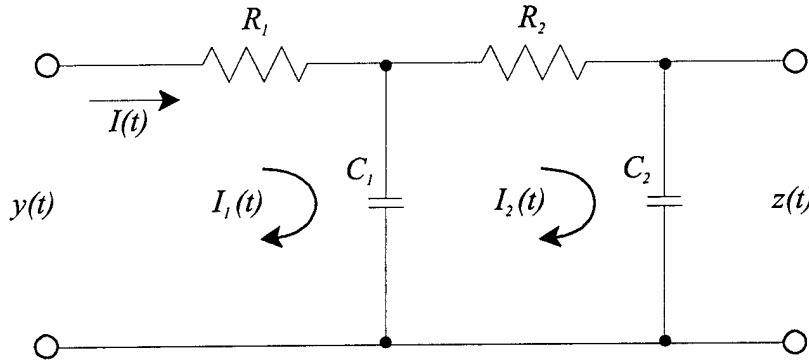


Figure 2-1 Schematic diagram of a two-pole lowpass filter used to isolate the I&Q components of the baseband radar signal.

An expression for the filter output voltage, $z(t)$, can be derived from Figure 2-1 using Kirchoff's rules and the relationship

$$I(t) = C \frac{dV(t)}{dt} \quad (6)$$

where C is the capacity (farads) of a capacitor,
 $I(t)$ is the time-varying current (amperes) through the capacitor, and
 $V(t)$ is the time-varying voltage applied across the capacitor.

The filter output voltage can be written as

$$z(t) = y(t) - (R_1(C_1 + C_2) + R_2C_2) \frac{dz(t)}{dt} - R_1C_1R_2C_2 \frac{d^2z(t)}{dt^2} \quad (7)$$

where R_1 , R_2 , C_1 , and C_2 represent the filter's resistors and capacitors, respectively.

Equation 7 can be rewritten in the form

$$(D^2 + 2\alpha D + b)z(t) = b y(t) \quad (8)$$

where $D \equiv \frac{d}{dt}$, which denotes differentiation by time,

$$2\alpha = \frac{R_1(C_1 + C_2) + R_2 C_2}{R_1 C_1 R_2 C_2}, \text{ and}$$

$$b = \frac{1}{R_1 C_1 R_2 C_2}.$$

Equation 8 can be solved for the filter output voltage, $z(t)$, by application of the Laplace Transform and the Convolution Theorem [2]. The filter output voltage becomes

$$z(t) = \frac{r_1 r_2}{r_1 - r_2} \left(e^{r_1 t} \int_0^t e^{-r_1 \xi} y(\xi) d\xi - e^{r_2 t} \int_0^t e^{-r_2 \xi} y(\xi) d\xi \right) \quad (9)$$

where r_1 and r_2 are the roots of the characteristic equation $s^2 + 2\alpha s + b = 0$ (note that $r_1 r_2 = b$), and ξ is a variable of integration.

Substituting Equations 4 and 5 into Equation 9 gives the filter output voltage, $z(t)$, as a function of the radar return signal, $x_n(t)$:

$$z(t) = \frac{r_1 r_2}{r_1 - r_2} \left(e^{r_1 t} \int_0^t e^{-(i\omega_0 + r_1)\xi} \sum_{n=1}^N x_n(\xi) d\xi - e^{r_2 t} \int_0^t e^{-(i\omega_0 + r_2)\xi} \sum_{n=1}^N x_n(\xi) d\xi \right) \quad (10)$$

By the definition of $x_n(t)$ given in Equations 1 and 2, the output due to the n^{th} input pulse can be shown to be

$$z_n(t) = \frac{r_1 r_2}{r_1 - r_2} \left(e^{r_1 t} \int_{t_n}^t e^{-(i\omega_0 + r_1)\xi} \sin(\omega\xi) d\xi - e^{r_2 t} \int_{t_n}^t e^{-(i\omega_0 + r_2)\xi} \sin(\omega\xi) d\xi \right), \quad t_n \leq t < t_{n+1} \quad (11)$$

where $t_n \equiv (n-1)T$.

The integrals in Equation 11 must be evaluated separately for two different time periods: during the pulse, $t_n \leq t < (t_n + \tau)$, and after the pulse, $(t_n + \tau) \leq t < t_{n+1}$. Evaluating the integrals is simplified by making the substitutions

$$t = t_n + t_r \quad (12)$$

and

$$\sin(\omega\xi) = \frac{e^{i(\omega_0 + \omega_D)\xi} - e^{-i(\omega_0 + \omega_D)\xi}}{2i} \quad (13)$$

where t_r is time relative to the start of the n^{th} pulse.

Substituting Equations 12 and 13 into Equation 11 and evaluating the integrals gives

$$z_n(t_r) = \begin{cases} \frac{1}{2i} \frac{r_1 r_2}{r_1 - r_2} \left(e^{r_1 t_r} \left[\frac{e^{i\omega_D t_n}}{a_1} (e^{a_1 t_r} - 1) + \frac{e^{-i(2\omega_0 + \omega_D)t_n}}{b_1} (e^{b_1 t_r} - 1) \right] - \right. \\ \left. e^{r_2 t_r} \left[\frac{e^{i\omega_D t_n}}{a_2} (e^{a_2 t_r} - 1) + \frac{e^{-i(2\omega_0 + \omega_D)t_n}}{b_2} (e^{b_2 t_r} - 1) \right] \right), & t_r < \tau \\ \frac{1}{2i} \frac{r_1 r_2}{r_1 - r_2} \left(e^{r_1 t_r} \left[\frac{e^{i\omega_D t_n}}{a_1} (e^{a_1 \tau} - 1) + \frac{e^{-i(2\omega_0 + \omega_D)t_n}}{b_1} (e^{b_1 \tau} - 1) \right] - \right. \\ \left. e^{r_2 t_r} \left[\frac{e^{i\omega_D t_n}}{a_2} (e^{a_2 \tau} - 1) + \frac{e^{-i(2\omega_0 + \omega_D)t_n}}{b_2} (e^{b_2 \tau} - 1) \right] \right), & t_r \geq \tau \end{cases} \quad (14)$$

where $a_1 \equiv (i\omega_D - r_1)$,
 $a_2 \equiv (i\omega_D - r_2)$,
 $b_1 \equiv -(i[2\omega_0 + \omega_D] + r_1)$, and
 $b_2 \equiv -(i[2\omega_0 + \omega_D] + r_2)$.

For the experimental air-to-air radar system, the pulse period is an integral number of pulse widths ($T = M\tau$) and the pulse width is four divided by the radar intermediate frequency ($\tau = 4/f_0$). This gives

$$e^{2i\omega_0 t_n} = e^{4\pi i f_0 (n-1)T} = e^{4\pi i f_0 (n-1)(4M/f_0)} = 1 \quad (15)$$

Substituting Equation 15 into Equation 14 and rearranging the terms gives

$$z_n(t_r) = \begin{cases} \frac{1}{2i} \frac{r_1 r_2}{r_1 - r_2} \left(\left[\frac{e^{r_1 t_r}}{a_1} (e^{a_1 t_r} - 1) - \frac{e^{r_2 t_r}}{a_2} (e^{a_2 t_r} - 1) \right] e^{i\omega_D t_n} + \right. \\ \left. \left[\frac{e^{r_1 t_r}}{b_1} (e^{b_1 t_r} - 1) - \frac{e^{r_2 t_r}}{b_2} (e^{b_2 t_r} - 1) \right] e^{-i\omega_D t_n} \right), & t_r < \tau \\ \frac{1}{2i} \frac{r_1 r_2}{r_1 - r_2} \left(\left[\frac{e^{r_1 t_r}}{a_1} (e^{a_1 \tau} - 1) - \frac{e^{r_2 t_r}}{a_2} (e^{a_2 \tau} - 1) \right] e^{i\omega_D t_n} + \right. \\ \left. \left[\frac{e^{r_1 t_r}}{b_1} (e^{b_1 \tau} - 1) - \frac{e^{r_2 t_r}}{b_2} (e^{b_2 \tau} - 1) \right] e^{-i\omega_D t_n} \right), & t_r \geq \tau \end{cases} \quad (16)$$

which is the filtered baseband pulse Doppler return signal (I&Q) from a point target.

2.3 TRANSIENT DOPPLER ARTIFACTS

Equation 16 shows that the filtered baseband pulse Doppler return signal (I&Q) from a point target consists of two terms: one term at the positive Doppler frequency (the $e^{i\omega_D t_n}$ term) and the other term at the negative Doppler frequency (the $e^{-i\omega_D t_n}$ term).

Equation 16 can be evaluated numerically using the MATLAB [3] program in Listing A-1. Figure 2-2 shows the relative power of the positive Doppler term (target) and the negative Doppler term (artifact) as functions of time for a 640 nanosecond radar pulse starting at time zero. The pulse location and pulse width are denoted in the figure by the shaded area. The figure shows that the artifact level reaches local maxima shortly after the leading and trailing edges of the pulse. The maximum artifact level associated with the leading edge of the pulse is 30.1 dB below the maximum target level, while the maximum artifact level associated with the trailing edge is 33.2 dB below the maximum target level. Note the fine structure of the leading edge transient.

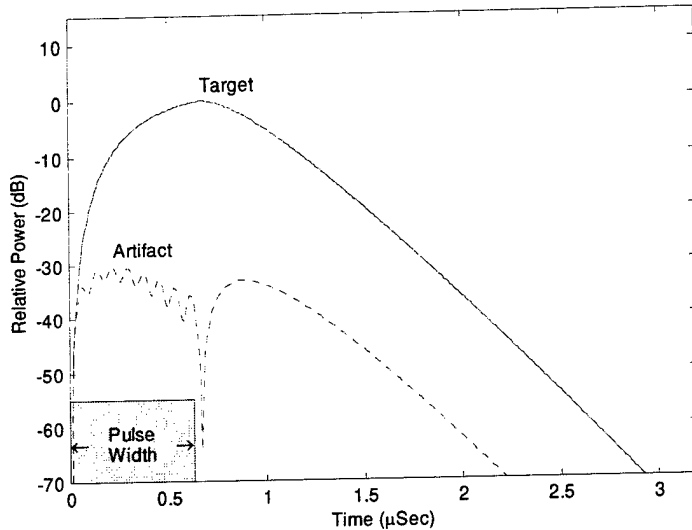


Figure 2-2 Relative power of the positive Doppler term (target) and the negative Doppler term (artifact) for a 640 nanosecond pulse. The pulse location and pulse width are denoted by the shaded region.

The maximum trailing edge artifact power level can be determined from the negative Doppler term (the $e^{-i\omega_D t_n}$ term) of Equation 16 by differentiating with respect to t , to find the time of the maximum power level, then substituting this time back into Equation 16. This substitution and some approximations give

$$P_{Max-}(t_r \geq \tau) \approx \left| \frac{r}{16\pi f_0} \right|^2 \quad (17)$$

where $r = r_1 \approx r_2$,

$r \gg \omega_D$, and

$\omega_0 \gg \omega_D$.

Equation 17 shows that the maximum artifact power level can be reduced by decreasing r , which corresponds to decreasing the filter bandwidth, or by increasing the radar intermediate frequency, f_0 . The MATLAB program in Listing A-1 evaluates Equation 17 to approximate the maximum trailing edge artifact power level; the numerical value is 28.7 dB below the maximum target level for the example shown above in Figure 2-2.

Figure 2-3 shows the relative power of the positive Doppler term (target) and the negative Doppler term (artifact) as functions of time for a 2 microsecond pulse starting at time zero. The pulse location and pulse width are denoted in the figure by the shaded area. The maximum leading edge artifact level is 31.9 dB below the maximum target level, while the maximum trailing edge artifact level is 33.2 dB below the maximum target level. The figure shows that the artifact power level decreases asymptotically during the pulse to some fixed level at the end of the pulse. This fixed level represents the steady-state rejection of the negative Doppler term by the lowpass filter. In this case, the filter rejection ratio is 49.1 dB.

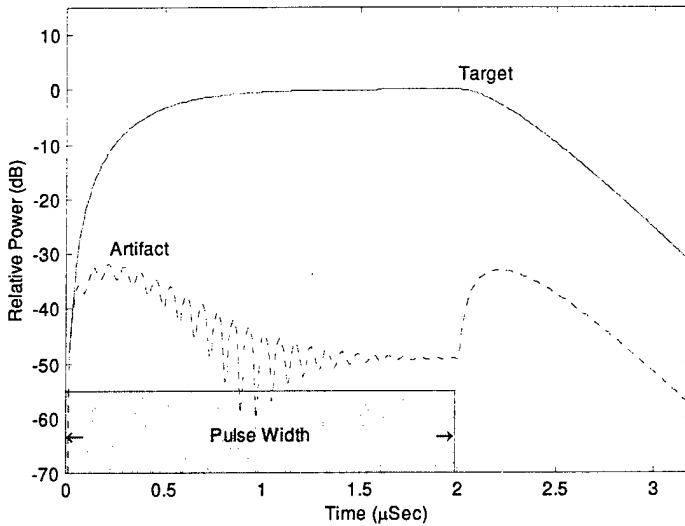


Figure 2-3 Relative power of the positive Doppler term (target) and the negative Doppler term (artifact) for a 2 microsecond pulse. The pulse location and pulse width are denoted by the shaded region.

From Equation 16, the ratio of the artifact to target power can be written as

$$R(t_r) = \begin{cases} \left| \frac{e^{r_1 t_r} (e^{b_1 t_r} - 1) - \frac{e^{r_2 t_r}}{b_2} (e^{b_2 t_r} - 1)}{b_1} \right|^2, & t_r < \tau \\ \left| \frac{e^{r_1 t_r} (e^{a_1 t_r} - 1) - \frac{e^{r_2 t_r}}{a_2} (e^{a_2 t_r} - 1)}{a_1} \right|^2, & \\ \left| \frac{e^{r_1 t_r} (e^{b_1 \tau} - 1) - \frac{e^{r_2 t_r}}{b_2} (e^{b_2 \tau} - 1)}{b_1} \right|^2, & t_r \geq \tau \\ \left| \frac{e^{r_1 t_r} (e^{a_1 \tau} - 1) - \frac{e^{r_2 t_r}}{a_2} (e^{a_2 \tau} - 1)}{a_1} \right|^2, & \end{cases} \quad (18)$$

The asymptotic power ratio at the end of the pulse can be approximated from the upper portion of Equation 18 by letting t_r become so large that the exponential terms $e^{r_1 t_r}$ and $e^{r_2 t_r}$ go to zero. The result is

$$R_1 \approx \left| \frac{r}{4\pi f_0} \right|^4 \quad (19)$$

where $r = r_1 \approx r_2$,

$r \gg \omega_D$, and

$\omega_0 \gg \omega_D$.

Equation 19 gives the rejection of the negative Doppler artifact by the lowpass filter when driven with a continuous sinusoidal signal. The filter rejection ratio can be increased by decreasing r , which corresponds to decreasing the filter bandwidth, or by increasing the intermediate frequency, f_0 . The filter rejection ratio is calculated by the MATLAB program in Listing A-1; the numerical value is 49.1 dB below the maximum target level for the example shown above in Figure 2-3.

3.0 SIMULATION RESULTS

This section presents a software simulation of the quadrature demodulation of the pulse Doppler return signal from a point target that was discussed in the previous section. The simulation produces a time-frequency image that exhibits transient Doppler artifacts similar to those predicted by the mathematical analysis.

The MATLAB program in Listing A-2 simulates the quadrature demodulation of the target return signal given by Equation 4. The target return signal is formed by computing a sinusoidal signal for the entire coherent processing interval and then applying a mask to each pulse period to simulate the radar pulses. The frequency of the sinusoidal signal is the radar intermediate frequency plus the Doppler frequency of the simulated target. (The choice of Doppler frequency is somewhat arbitrary; a value of 0.25 times the pulse repetition frequency has been selected, as it provides for the greatest separation in frequency between the target and the artifact, and also ensures that the target and artifact signals are centered in a Doppler frequency bin.) The pulsed sinusoidal signal is multiplied by the complex exponential of the radar intermediate frequency and then lowpass filtered using an Infinite Impulse Response approximation of the two-pole lowpass filter shown in Figure 2-1 and analyzed in Section 2.2.

The time-frequency image produced by the software simulation is shown in Figure 3-1. The figure shows the power level (in decibels) of the simulated target return and the artifact as a function of the time from the start of the pulse (horizontal axis) and the Doppler frequency (vertical axis). The pulse location and pulse width are denoted by the shaded region. The image shows clearly the separation in time between the leading edge artifact and the trailing edge artifact. The maximum level of the leading edge artifact is 30.0 dB below the maximum target level; the maximum level of the trailing edge artifact is 32.9 dB below the maximum target level. The artifact is located at a Doppler frequency that is the negative of the target Doppler frequency.

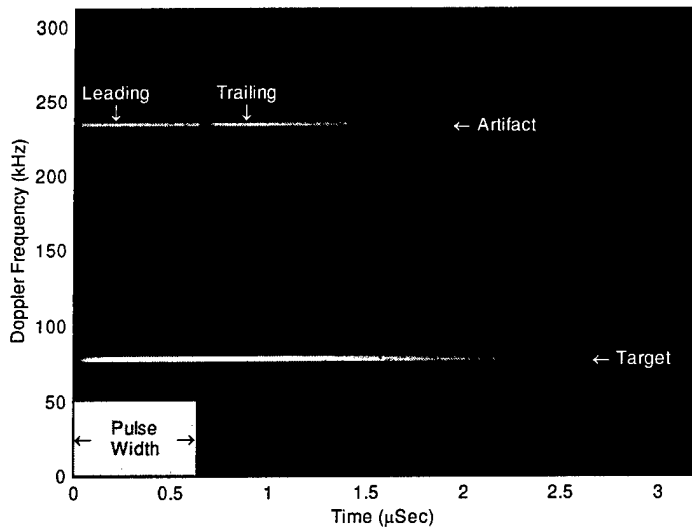


Figure 3-1 Time-Frequency image produced by the software simulation, showing the power level of the simulated target return and the artifact as a function of time and frequency. The pulse location and pulse width are denoted by the shaded region.

Figure 3-2 shows cross sections in time through the simulated target and the artifact shown above in Figure 3-1. The pulse location and pulse width are denoted by the shaded region. These curves are to be compared with those shown previously in Figure 2-2; the root-mean-square difference between the relative artifact power levels is less than 1 dB.

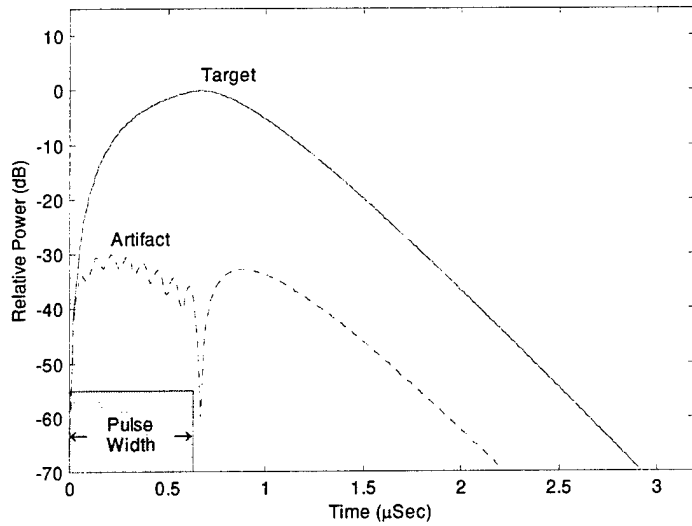


Figure 3-2 Cross-sections in time through the simulated target and the artifact for the software simulation. The pulse location and pulse width are denoted by the shaded region.

4.0 EXPERIMENTAL RESULTS

This section presents experimental results obtained from measurements of a synthetic target signal applied to the Digital Radar Receiver, which implements quadrature demodulation in hardware. The experimental results confirm the existence of transient Doppler artifacts consistent with both the mathematical analysis in Section 2.0 and the software simulation in Section 3.0.

4.1 HARDWARE DESCRIPTION

Figure 4-1 shows a block diagram of the Digital Radar Receiver, which is implemented as two cards in a VME-based system. The Digital Radar Receiver uses a Pentek Model 6441 Analog-to-Digital Converter VME Board [4] to digitize the radar signal at the intermediate frequency, and a modified Pentek Model 4272 Multiband Digital Receiver Module [5] to downconvert and band limit the wideband radar data.

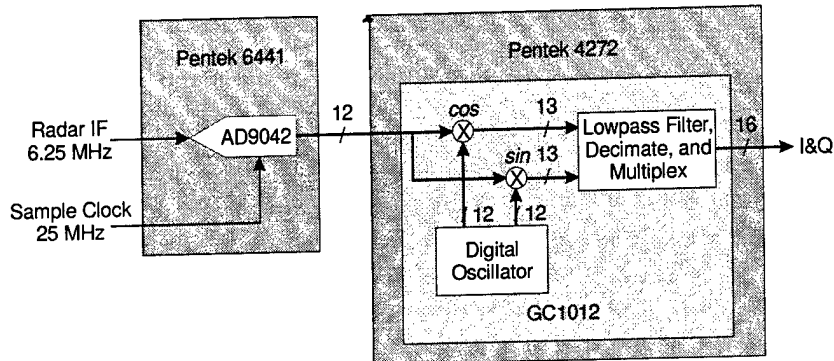


Figure 4-1 Block diagram of the Digital Radar Receiver hardware.

The Analog-to-Digital Converter Board samples the input signal with 12-bit resolution at a sample rate of 25 MHz, which is four times the radar intermediate frequency of 6.25 MHz. The maximum signal amplitude is 2.0 volts peak-to-peak. The output of the analog-to-digital converter is sent to the wideband input port of the Multiband Digital Receiver Module. This port uses a Graychip GC1012 Digital Tuner Chip [6] to process the sampled input signal. The GC1012 first multiplies the input data by *cosine* and *sine* sequences tuned to the radar intermediate frequency. The product sequences are lowpass filtered and decimated (sub-sampled) by a factor of 16, reducing the output data rate to 1.5625 MHz. The decimated data sequences are rounded and multiplexed to form the complex In-phase and Quadrature-phase (I&Q) data stream that is analogous to the output voltage, $z(t)$, of the lowpass filter discussed in Section 2.2.

The output sample period, which is the reciprocal of the output data rate, is 640 nanoseconds. This period corresponds to the *range cell* or *range bin* of an analog radar receiver [7] and is referred to here as the *range gate*. This period defines the range resolution of the radar, which is approximately 96 meters.

4.2 MEASUREMENTS

The synthetic target signal is a pulsed sinusoid of fixed amplitude at a frequency that is the sum of the radar intermediate frequency (6.25 MHz) and the target Doppler frequency. For the measurements presented here, the Doppler frequency is 3 kHz, the pulse width is 640 nanoseconds, and the pulse repetition frequency is 16.6 kHz.

A range-Doppler map is an image that is formed by grouping the I&Q radar data for a coherent processing interval into a matrix of N pulse periods by M range gates. A complex Fast Fourier Transform is applied to the N I&Q samples at each range gate, transforming the time domain data into the frequency domain. The frequency domain data are squared and converted to decibels to represent the power of the radar signal as a function of range gate (horizontal axis) and Doppler frequency (vertical axis).

The range-Doppler map is ambiguous in both range gate and Doppler frequency. Given a target with unambiguous range gate and Doppler frequency coordinates (m, f_D) , the apparent range gate and Doppler frequency coordinates will be $(m \bmod M, f_D \bmod PRF)$. For example, the artifact associated with the synthetic target signal will appear in the range-Doppler map with a Doppler frequency of $(-3.0 \text{ kHz} \bmod 16.6 \text{ kHz})$, which is 13.6 kHz .

The range-Doppler map computed from the I&Q output of the Digital Radar Receiver due to application of the synthetic target signal is shown in Figure 4-2. The figure indicates the locations of the synthetic target at the expected Doppler frequency of 3.0 kHz , and the artifact at the negative Doppler frequency of -3.0 kHz , which is aliased to 13.6 kHz . The dynamic range of the image is 90 dB . The maximum power level of the artifact is 30 dB below the maximum power level of the synthetic target.

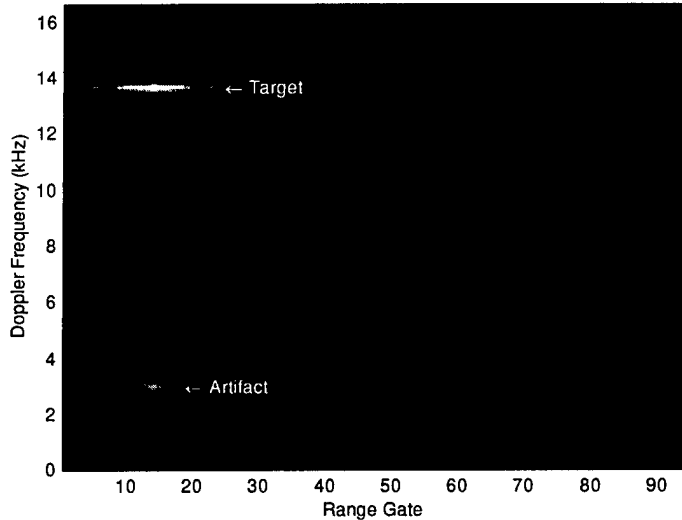


Figure 4-2 Range-Doppler map computed from the output of the Digital Radar Receiver due to application of the synthetic target signal, showing the locations of the synthetic target and the artifact.

5.0 IMPACT ON RADAR PERFORMANCE

This section discusses the potential impact of the transient Doppler artifacts on the detection performance of a radar system, and considers techniques to mitigate the deleterious effects of the artifacts.

5.1 OPERATIONAL IMPACT

The air-to-air surveillance mode for the CP-140 will normally operate in a down-looking mode. That is, the CP-140 will normally fly above any potential targets, with the radar antenna pointing down, scanning

a volume of airspace for targets. There will be a strong return signal from the portion of the earth's surface that is illuminated by the main lobe of the antenna. This signal is called the main lobe clutter.

As an example, Figure 5-1 shows a range-Doppler map of simulated main lobe clutter generated by the *SAFIRE* radar simulation program. The scenario is that of a CP-140 flying at a altitude of 3,000 meters (about 10,000 feet) and at a speed of 180 meters per second (about 350 knots). The antenna is pointing at -3.3 degrees elevation (3.3 degrees down from the horizon) and 77.8 degrees azimuth (77.8 degrees clockwise from straight ahead). The pulse repetition frequency is 9.9 kHz and the radar pulse width is 600 nanoseconds. The broad band of energy spread over Doppler frequencies from about 2 kHz to about 3.2 kHz is the main lobe clutter. In general, targets that are masked by the main lobe clutter cannot be detected by a pulse Doppler radar.

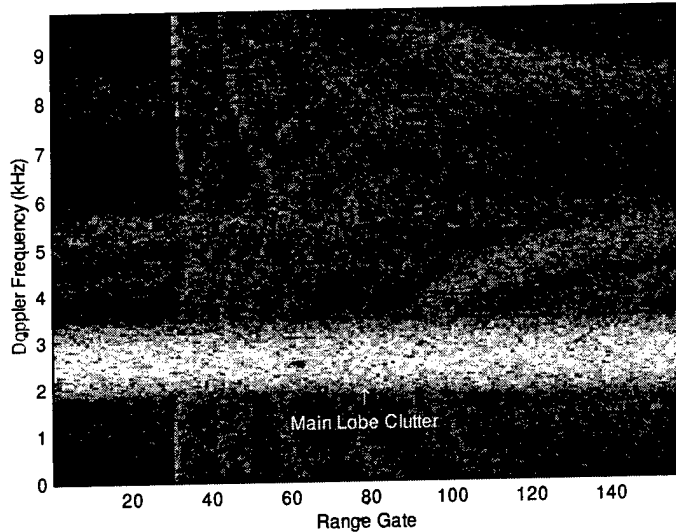


Figure 5-1 Range- Doppler map of simulated main lobe clutter generated by the *SAFIRE* radar simulation program.

The effect of the transient Doppler artifacts can be approximated for a range-Doppler map by inverting the range-Doppler matrix along the Doppler frequency axis, multiplying by the artifact-to-signal ratio, and adding the result to the original data matrix. Figure 5-2 shows the result of applying this process to the range-Doppler map shown in Figure 5-1, for an artifact-to-signal ratio of -30 dB. The artifact associated with the main lobe clutter is spread over Doppler frequencies from about 6.8 kHz to about 8 kHz. Weak radar targets located in that frequency band might be masked by the artifact. The artifact could effectively double the number of range-Doppler cells in which a target might be masked by the main lobe clutter.

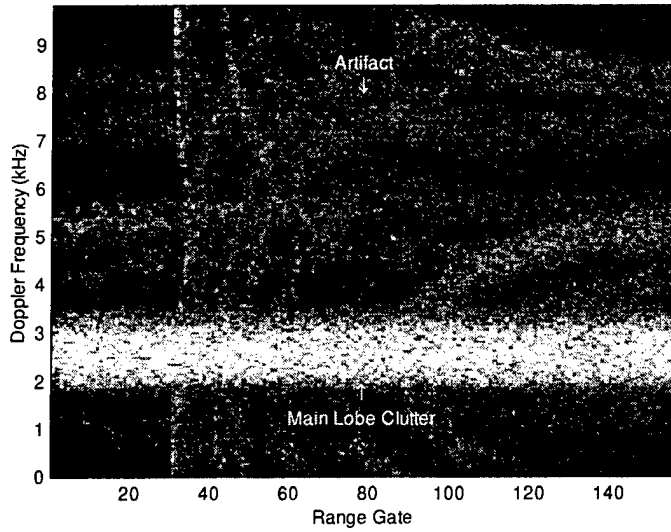


Figure 5-2 Range-Doppler map of simulated main lobe clutter with the addition of approximated transient Doppler artifacts.

5.2 MITIGATION OF EFFECT

5.2.1 VARIABLE FREQUENCY OSCILLATOR

The Variable Frequency Oscillator (VFO) tunes the quadrature demodulation of the radar return signal to the sum of the radar intermediate frequency and an estimate of Doppler frequency of the main lobe clutter. This effectively tunes the main lobe clutter to zero Doppler frequency in the range-Doppler map. This technique is often used in pulse Doppler radar systems to simplify subsequent target detection processing. In the present context, the Variable Frequency Oscillator will also tune the transient Doppler artifact of the main lobe clutter to zero Doppler frequency, eliminating the deleterious effects of the artifact associated with the main lobe clutter.

5.2.1.1 Target Scenario

Figure 5-3 shows the range-Doppler map of the scenario described above, this time with the addition of thermal noise and a target. The target is at a range of 48.2 kilometers (26 nautical miles), an altitude of 395 meters (1300 feet), and has a closing speed of 112 meters per second (218 knots). The radar cross section is 5 square meters.

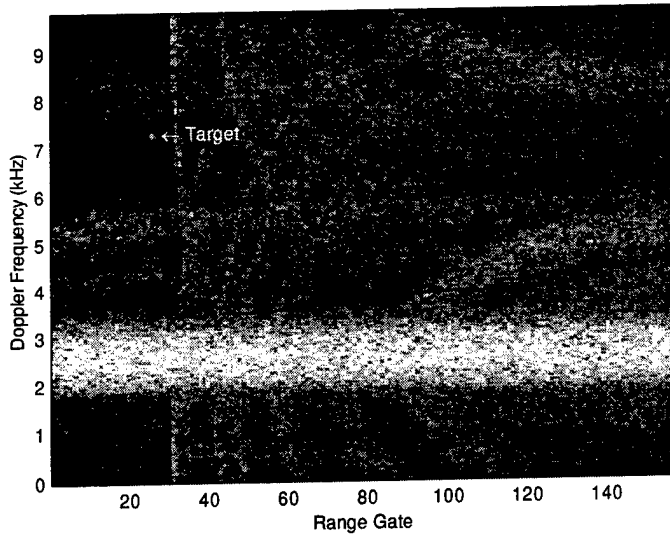


Figure 5-3 Range-Doppler map showing simulated main lobe clutter, thermal noise, and a target at a range of 48.2 kilometers.

Figure 5-4 shows cross sections in Doppler frequency and range gate through the target in Figure 5-3. While the target return is not as strong as the main lobe clutter, it is stronger than the surrounding clutter, with a local signal-to-noise ratio of about 26 dB.

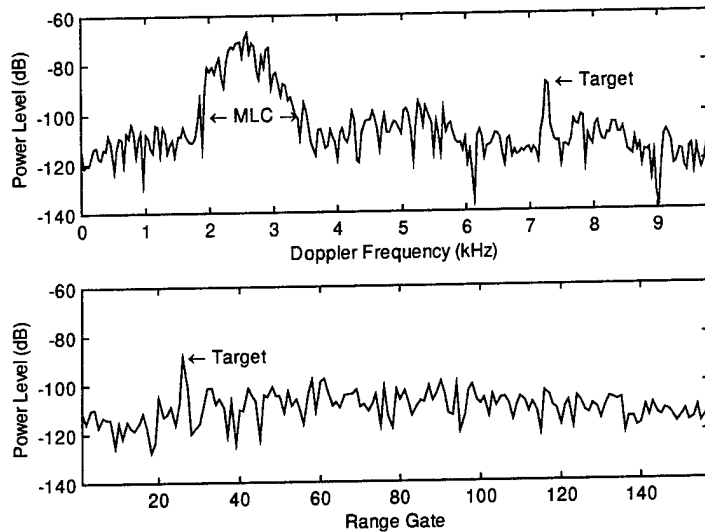


Figure 5-4 Cross sections in Doppler frequency (upper plot) and range gate (lower plot) through the target in Figure 5-3.

5.2.1.2 VFO Off

Adding an approximation of the transient Doppler artifact to the range-Doppler map shown in Figure 5-3 results in the range-Doppler map shown Figure 5-5. The artifact-to-signal ratio is -30 dB. The figure

shows that while the target is still visible, it is partially masked by the transient Doppler artifact of the main lobe clutter.

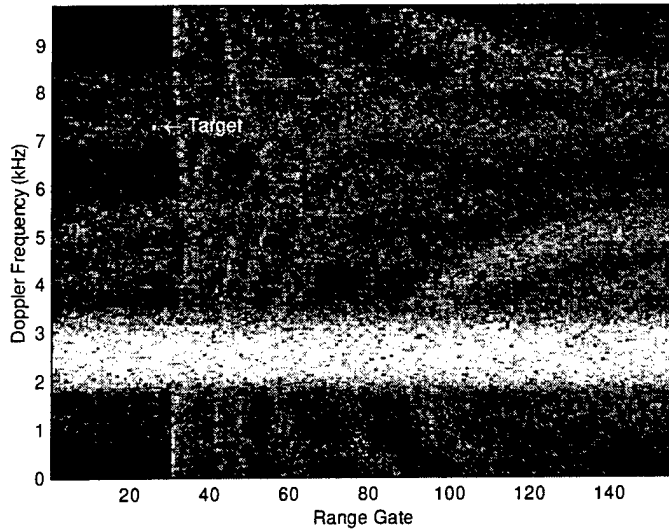


Figure 5-5 Range-Doppler map showing the simulated main lobe clutter, thermal noise, and a target, with approximated transient Doppler artifacts (VFO off).

Figure 5-6 shows cross sections in Doppler frequency and range gate through the target in Figure 5-5. The target is still stronger than the surrounding clutter and is still detectable, but the local signal-to-noise ratio has decreased to about 15 dB. This 11 dB reduction in signal-to-noise ratio in the region of the transient Doppler artifact would significantly reduce the detection performance of the radar.

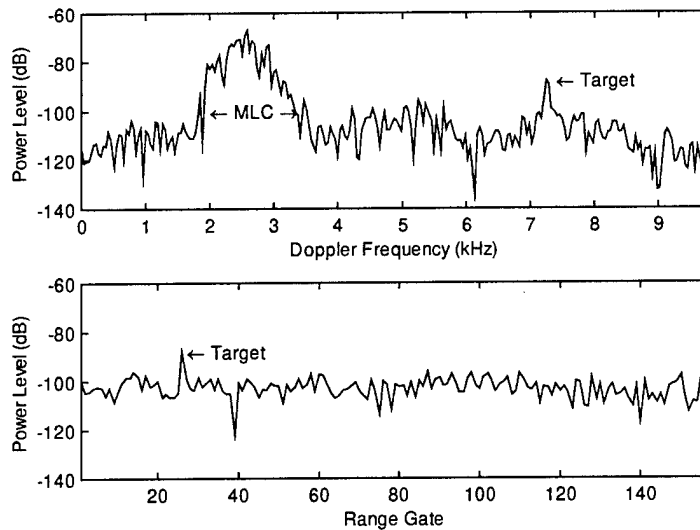


Figure 5-6 Cross sections in Doppler frequency (upper plot) and range gate (lower plot) through the target in Figure 5-5 (VFO Off).

5.2.1.3 VFO On

In contrast to the range-Doppler map shown Figure 5-5, Figure 5-7 shows the target and main lobe clutter with the simulated transient Doppler artifacts but now with the VFO turned on. Both the main lobe clutter and its artifact are mapped to zero Doppler frequency, and the target is not masked by the artifact.

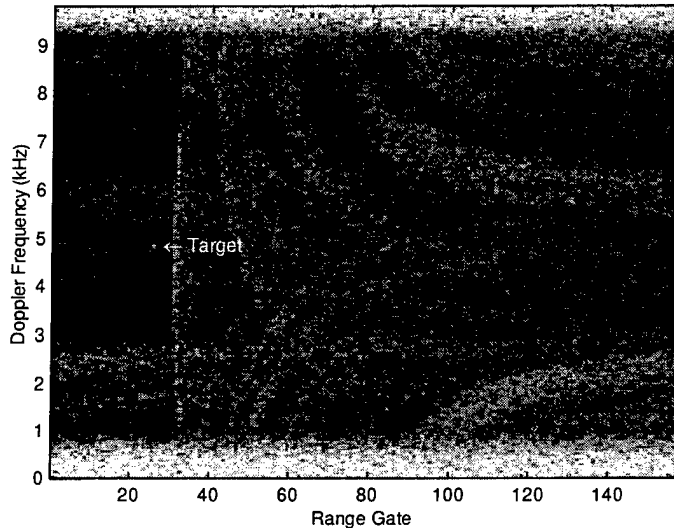


Figure 5-7 Range-Doppler map showing the simulated main lobe clutter, thermal noise, and a target, with approximated transient Doppler artifacts (VFO on).

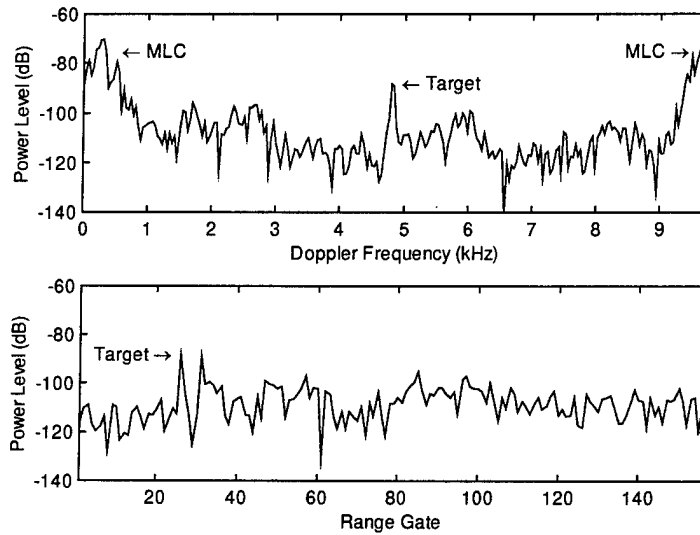


Figure 5-8 Cross sections in Doppler frequency (upper plot) and range gate (lower plot) through the target in Figure 5-7 (VFO on).

Figure 5-8 shows cross sections in Doppler frequency and range gate through the target in Figure 5-7. The target is stronger than the surrounding clutter and is detectable, with a local signal-to-noise ratio of about 26 dB. This is the same as the local signal-to-noise for the case of no artifacts and no VFO shown above

in Figure 5-3 and Figure 5-4. The VFO can be expected, therefore, to eliminate the degradation of detection performance due to masking of the target by the transient Doppler artifact associated with the main lobe clutter.

5.2.2 PULSE SHAPE

The transient Doppler artifact is shown in Section 2.0 to be associated with the leading and trailing edges of the pulse Doppler waveform. The strength of the artifact might be less for radar pulses having non-zero rise and fall times. The pulse Doppler waveform seen at the input of the analog-to-digital converter will typically have rise and fall times on the order of 50 to 100 nanoseconds.

The MATLAB program in Listing A-2 can accommodate symmetric linear rise and fall times for the radar pulses. Figure 5-9 shows the range-Doppler map of the simulated target and its transient Doppler artifact for pulses with rise and fall times of 80 nanoseconds. The maximum leading edge artifact power level is 41.3 dB below the maximum target level; the maximum trailing edge power level is 48.3 dB below the maximum target level. This is an improvement of 10 to 15 dB in the relative power levels of the transient Doppler artifact compared to the simulation results in Section 3.0 where the pulses have zero rise and fall times.

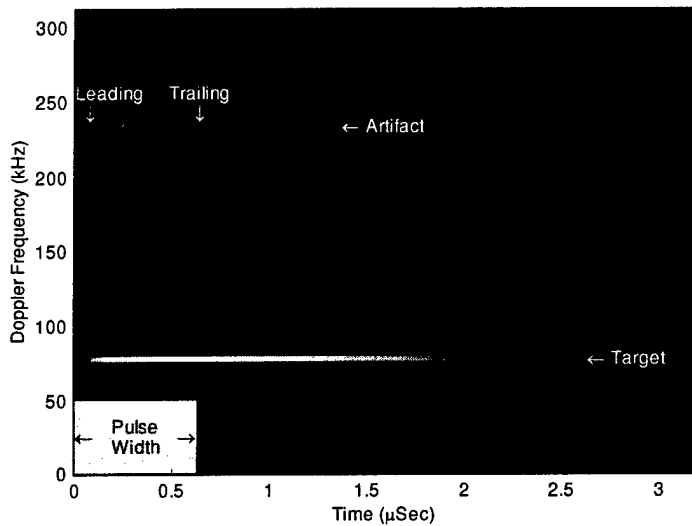


Figure 5-9 Time-Frequency image showing reduced transient Doppler artifacts for pulses with 80 nanosecond rise and fall times.

5.2.3 INCREASED INTERMEDIATE FREQUENCY

The analysis in Section 2.0 shows that the relative power level of the transient Doppler artifact can be reduced by decreasing the bandwidth of the lowpass filter or by increasing the radar intermediate frequency. The bandwidth of the lowpass filter is determined by other constraints such as optimizing the signal to noise ratio. In the case of the Digital Radar Receiver, the bandwidth of the lowpass filter is determined by the decimation factor and cannot be changed.

The choice of radar intermediate frequency is limited by the sample rate of the analog-to-digital converter. In the case of the Digital Radar Receiver, the maximum sample rate is limited to 41 MHz. The

design concept requires that the intermediate frequency be one-quarter the sample rate. This gives a maximum intermediate frequency of 10.25 MHz, and a potential reduction of 4 dB in artifact level.

Using data derived from the MATLAB program in Listing A-1, Table 5-1 summarizes the expected transient Doppler artifact power levels relative to the maximum target level for a number of different intermediate frequencies.

Table 5-1 Relative artifact power level for various intermediate frequencies.

Intermediate Frequency (MHz)	Relative Leading Artifact Power Level (dB)	Relative Trailing Artifact Power Level (dB)
6.25	30.1	33.1
12.5	36.8	39.1
25.0	43.1	45.1
50.0	49.3	51.1
100.0	55.4	57.2
200.0	61.4	63.2
400.0	67.5	69.2

Future designs could take advantage of faster hardware as it becomes available. With sufficiently capable hardware, the intermediate frequency could eventually reach the 50 MHz to 100 MHz region typically used in analog radar systems. An intermediate frequency of 100 MHz would require an analog-to-digital converter with a sample rate of 400 MHz or higher, but would result in an improvement of about 25 dB in artifact level.

6.0 SUMMARY AND CONCLUSIONS

This report has presented a mathematical analysis of the pulse Doppler return signal expected from a point target. The analysis predicts the existence of transient Doppler artifacts associated with the leading and trailing edges of the radar pulses. The maximum power level of the artifacts, relative to the maximum power level of the target signal, is shown to be inversely proportional to the square of the radar intermediate frequency. For the experimental air-to-air radar, the analysis predicts an artifact power level about 30 dB less than the target signal level, with the artifact occurring at a frequency that is the negative of the target signal Doppler frequency.

Quadrature demodulation of the pulse Doppler return signal from a point target is simulated in software. The simulation produces a time-frequency image that exhibits transient Doppler artifacts similar to those predicted by the mathematical analysis. The maximum power level of the simulation artifact is about 27 dB less than the simulated target level. The simulation artifact appears in the time-frequency image at a frequency that is the negative of the target Doppler frequency.

A Range-Doppler map derived from experimental measurements of a synthetic target signal applied to the Digital Radar Receiver exhibits transient Doppler artifacts consistent with both the mathematical analysis and the software simulation. The maximum power level of the experimentally measured artifact is about 25 dB less than the synthetic target level. The experimentally measured artifact appears in the Range-Doppler map at a frequency that is the negative of the synthetic target Doppler frequency.

Using the SAFIRE radar simulation program, a simulation of the main lobe clutter expected in CP-140 operations indicates that the transient Doppler artifacts could degrade the signal to noise ratio of targets

by about 10 dB if the target falls in the frequency band occupied by the artifact associated with the main lobe clutter. The detection performance of a radar system would be degraded under these conditions.

Techniques to mitigate the deleterious effects of the artifacts include using a Variable Frequency Oscillator, using pulses with non-zero rise and fall times, and increasing the radar intermediate frequency. The Variable Frequency Oscillator tunes the Doppler frequency of the main lobe clutter and its artifact both to zero. This preserves the local signal to noise ratio for the target, and thereby eliminates the effect of the transient Doppler artifact associated with the main lobe clutter. Using radar pulses with non-zero rise and fall times, as would be the case with any real radar transmitter, further reduces the relative power level of the transient Doppler artifacts. For example, using pulses with rise and fall times of 80 nanoseconds reduces the relative artifact power level by 10 to 15 dB. Future systems could take advantage of faster hardware as it becomes available, with the goal of eventually increasing the intermediate frequency to about 100 MHz. This would require an analog-to-digital converter capable of sampling at 400 MHz, but would reduce the artifact power level by about 25 dB.

Combining pulses with non-zero rise and fall times with an intermediate frequency of 100 MHz could reduce the maximum artifact power level to 65 to 70 dB below the maximum signal power level. This is approaching the noise floor of the radar receiver; it would be difficult even to detect the transient Doppler artifacts at this power level, and they would have little or no impact on system performance.

APPENDIX A. MATLAB PROGRAMS

This appendix lists the MATLAB programs referenced in the main body of the report. MATLAB is a language for technical computing published by The MathWorks, Inc. of Natick, Massachusetts. The language is particularly suited for vector and matrix arithmetic, and for graphical rendering of numeric information.

Listing A-1 MATLAB program to calculate the filtered baseband pulse Doppler radar return signal from a point target

```
function artifact = artifact1(pw,mult)
%ARTIFACT1 evaluates the analytic expression in Equation 16
%
%artifact = artifact1(pw,mult)
%
%Input:
%    pw = width of radar pulse [default = 640e-9]
%    mult = multiplier for higher Intermediate Frequencies [default = 1]
%
%Output:
%    artifact = relative artifact power
%
%For Figure 2.2 use: >> artifact1;
%    Figure 2.3 use: >> artifact1(2e-6);
%    Table 5.1 use:  >> artifact1(640e-9,mult); mult = 1, 2, 4, 8, 16, 32, 64

% Steven Hughes
% DREO/ARN
% Last edit: 01 Dec 1999

% Set default values for the input parameters
if nargin < 2
    mult = 1;
    if nargin < 1
        pw = 640e-9;
    end
end

% Check that the IF multiplier is a positive integer
if mult < 1 | floor(mult) ~= mult
    error('The IF multiplier must be a positive integer.');
end

% Set the radar Intermediate Frequency
f0 = mult*6.25e6;      % basic radar IF is 6.25 MHz
w0 = 2*pi*f0;          % angular IF

% Set the sample rate high enough to resolve the fine structure
% of the leading edge artifact
fs = 16*f0;             % sample rate

% Set the pulse repetition interval (PRI) long enough to capture
% the decay of the trailing edge artifact
T = mult*20/f0;          % pulse period (PRI)
```

```

% Set the Doppler frequency of the target. The actual Doppler frequency
% is somewhat arbitrary: choose 1/4 of the PRF.
prf = 1/T; % pulse repetition frequency
fD = prf/4.0; % target Doppler frequency
wD = 2*pi*fD; % angular Doppler

% Compute the number of samples in the pulse and in the pulse period
pw_samples = round(pw*fs); % # samples in the pulse
pri_samples = round(T*fs); % # samples in a pulse period

% These are the roots (poles) for the two-pole RC filter
% matched to a 640 ns pulse
r1 = -4660712;
r2 = -4660720;

% Compute the parameters used to evaluate Equation 16
a1 = i*wD - r1;
a2 = i*wD - r2;
b1 = -(i*(2*w0+wD) + r1);
b2 = -(i*(2*w0+wD) + r2);

rs = r1*r2/(2*i*(r1-r2));

% Evaluate Equation 16 during the pulse
tr = (0:pw_samples-1)/fs;
target = rs*term(r1,a1,r2,a2,tr,tr);
artifact = rs*term(r1,b1,r2,b2,tr,tr);

% Evaluate Equation 16 after the pulse and append to the above
tr = (pw_samples:pri_samples-1)/fs;
target = [target rs*term(r1,a1,r2,a2,tr,pw)];
artifact = [artifact rs*term(r1,b1,r2,b2,tr,pw)];

% Convert to dB for plot
% - add 'realmin' to stop MATLAB complaining about taking logarithms of zero
target = 20*log10(abs(target)+realmin);
artifact = 20*log10(abs(artifact)+realmin);

% Plot the relative target and artifact power levels
time = (0:pri_samples-1)/fs*1e6; % time in microseconds
plot(time,target-max(target));
hold on
% - shade in the pulse time
xfill = [time(1) time(1:pw_samples) time(pw_samples)];
yfill = [-70 0*artifact(1:pw_samples)-55 -70];
fill(xfill,yfill,'y');
plot(time,artifact-max(target),':');
hold off
axis([0 max(time) -70 15]);
% - label the plot
ix = find(target == max(target));
ix = ix(1);
text(time(ix),3,'Target');
ix = find(artifact == max(artifact));
ix = ix(1);

```

```

text(time(ix),max(artifact)-max(target)+3,'Artifact');
xlabel('Time (\mu Sec)');
ylabel('Relative Power (dB)');
if pw < 0.8e-6
    text(time(pw_samples)/2,-63,'Pulse',...
        'HorizontalAlignment','Center','VerticalAlignment','Bottom');
    text(time(pw_samples)/2,-63,'Width',...
        'HorizontalAlignment','Center','VerticalAlignment','Top');
else
    text(time(pw_samples)/2,-63,'Pulse Width',...
        'HorizontalAlignment','Center','VerticalAlignment','Middle');
end
text(time(1),-63,'<arrow',...
    'HorizontalAlignment','Left','VerticalAlignment','Middle');
text(time(pw_samples),-63,'>arrow',...
    'HorizontalAlignment','Right','VerticalAlignment','Middle');

% Compute the relative power levels
max_leading = max(artifact(1:pw_samples));
max_trailing = max(artifact(pw_samples+1:pri_samples));
fprintf(1,'The target to leading artifact ratio is %.1f dB.\n',...
    max(target)-max_leading);
if mult > 1
    fprintf(1,'-- this is an improvement of %.1f dB.\n',...
        max(target)-max_leading - 30.1);
end
fprintf(1,'The target to trailing artifact ratio is %.1f dB.\n',...
    max(target)-max_trailing);
if mult > 1
    fprintf(1,'-- this is an improvement of %.1f dB.\n',...
        max(target)-max_trailing - 33.1);
end

% Compute the approximate power ratio for the trailing artifact
% according to Equation 17
r = (r1 + r2)/2;
PMax = 20*log10(abs(r/(16*pi*f0)));
fprintf(1,'The approximate trailing artifact power ratio is %.1f dB.\n',...
    max(target)-PMax);

if pw >= 1.75e-6
    % Compute the approximate asymptotic power ratio for the mid-pulse artifact
    % according to Equation 19 (this makes sense only for long pulses)
    R1 = 40*log10(abs(r/(4*pi*f0)));
    fprintf(1,'The approximate filter rejection ratio is %.1f dB.\n',...
        -R1);
    fprintf(1,'The simulated filter rejection ratio is %.1f dB.\n',...
        max(target)-artifact(pw_samples));
end

artifact = artifact - max(target);

return;
%%%%%%%%%%%%%%%

```

```

%
% Compute the inner term in Equation 16
% - the calling program changes the parameters to evaluate the target and
% artifact terms both during and after the pulse
function x = term(r1,a1,r2,a2,t1,t2)
x = exp(r1*t1).* (exp(a1*t2)-1)/a1 - exp(r2*t1).* (exp(a2*t2)-1)/a2;
return;

```

Listing A-2 MATLAB program to simulate the quadrature demodulation of a pulse Doppler radar return signal from a point target

```

function artifact = artifact2(rise)
%ARTIFACT2 simulates the demodulation of the pulse Doppler return signal
%
%artifact = artifact2
%
%Input:
%    rise = rise/fall time (seconds) [default = 0]
%
%Output:
%    artifact = relative artifact power
%
%For Figures 3.1 and 3.2 use: >> artifact2;
%For Figure 5.9 use: >> artifact2(80e-9);

% Steven Hughes
% DREO/ARN
% Last edit: 01 Dec 1999

% Set the default input parameters
if nargin < 1
    rise = 0.0;
end
if rise < 0.0
    error('The pulse rise/fall time must be greater than 0.');
end

% Set the pulse width
pw = 640e-9;

% Set the radar Intermediate Frequency
f0 = 6.25e6;           % radar IF is 6.25 MHz
w0 = 2*pi*f0;          % angular IF

% Set the sample rate
fs = 16*f0;            % sample rate

% Set the pulse repetition interval (PRI) long enough to capture
% the decay of the trailing edge artifact
T = 20/f0;              % pulse period (PRI)

% Set the Doppler frequency of the target. The actual Doppler frequency
% is somewhat arbitrary: choose 1/4 of the PRF.
prf = 1/T;               % pulse repetition frequency
fD = prf/4.0;             % target Doppler frequency

```

```

wD = 2*pi*fD;           % angular Doppler

% Compute the number of samples in the pulse and in the pulse period
pw_samples = round(pw*fs);    % # samples in the pulse
pri_samples = round(T*fs);    % # samples in a pulse period

% Compute the number of samples in a 256-pulse CPI
pulses = 256;
cpi_samples = pulses*pri_samples;  % # samples in a CPI

% Form the CW radar signal for an entire CPI
t = (0:cpi_samples-1)/fs;          % time for each sample in the CPI
x = sin((w0+wD)*t);              % the CW radar signal for the entire CPI

% Create the pulse mask
x = reshape(x,pri_samples,pulses); % reshape to a matrix
mask = zeros(pri_samples,1);        % initialize pulse mask to zero
mask(1:pw_samples) = 1;            % pulse mask

% - apply rise & fall times
if rise > 0.0
    n = round(rise*fs);          % number of samples in rise/fall time
    mask(1:n) = (0:n-1)/(n-1);
    mask(pw_samples-n+1:pw_samples) = (n-1:-1:0)/(n-1);
end

% Apply the pulse mask
for p = 1:pulses
    x(:,p) = x(:,p) .* mask;      % apply the mask for each pulse
end
x = reshape(x,1,cpi_samples);      % reshape back to a vector

% Mix to baseband
y = x .* exp(i*w0*t);            % complex quadrature data

% Define an IIR approximation to the two-pole RC filter
r1 = -4660712;      % roots (poles) for a 640 ns pulse
r2 = -4660720;

denom = ((2*fs-r1)*(2*fs-r2));
b(1) = r1*r2/denom;
b(2) = 2*b(1);
b(3) = b(1);

a(1) = 1;
a(2) = 2*(r1*r2-(2*fs)^2)/denom;
a(3) = ((2*fs+r1)*(2*fs+r2))/denom;

% Low-pass filter to isolate the baseband
z = filter(b,a,y);            % z contains the I&Q data

% Display the time-frequency data (Figure 3.1 or 5.9)
z = reshape(z,pri_samples,pulses)'; % reshape to a matrix
window = hanning(pulses);
for j=1:pri_samples

```

```

z(:,j) = window .* z(:,j);
end

cw = abs(fft(z)); % convert to frequency space
db = 20*log10(cw+realmin); % convert to dB scale
mdb = max(max(db)); % max value for display

levels = 80; % number of levels for display
colormap(gray(abs(levels))); % set the levels
x = (0:pri_samples-1)/fs*1e6; % time in microseconds
y = (0:pulses-1)/pulses*prf/1000; % frequency in kHz
image(x,y,db-mdb+levels), axis xy; % plot the time-Doppler map
xlabel('Time (\mu Sec)');
ylabel('Doppler Frequency (kHz)');

% Annotate the plot
% - point to the target
[jft,jt] = find(db == mdb); % location of maximum level (target)
target = db(jft,:); % the target cross section
j = find(target(jt+1:end)-max(target) < -60) + jt;
text(x(j(1)),y(jft),'\leftarrow Target','HorizontalAlignment','Left',...
    'VerticalAlignment','Middle','Color','white');
jfa = pulses + 2 - jft; % frequency index of artifact
artifact = db(jfa,:); % the artifact cross section
% - point to the leading and trailing artifacts
jlead = find(artifact(1:pw_samples) == max(artifact(1:pw_samples)));
text(x(jlead),y(jfa),'\downarrow','HorizontalAlignment','Center',...
    'VerticalAlignment','Bottom','Color','white');
if rise <= 0
    text(x(jlead),y(jfa)+15,'Leading','HorizontalAlignment','Center',...
        'VerticalAlignment','Bottom','Color','white');
else
    text(x(1),y(jfa)+15,'Leading','HorizontalAlignment','Left',...
        'VerticalAlignment','Bottom','Color','white');
end
jtrail = find(artifact(pw_samples+1:end) == ...
    max(artifact(pw_samples+1:end))) + pw_samples;
text(x(jtrail),y(jfa),'\downarrow','HorizontalAlignment','Center',...
    'VerticalAlignment','Bottom','Color','white');
text(x(jtrail),y(jfa)+15,'Trailing','HorizontalAlignment','Center',...
    'VerticalAlignment','Bottom','Color','white');
% - point to the artifact
j = find(artifact(jtrail+1:end)-max(target) < -60) + jtrail;
text(x(j(1)),y(jfa),'\leftarrow Artifact','HorizontalAlignment','Left',...
    'VerticalAlignment','Middle','Color','white');

hold on
xfill = [0 0 x(pw_samples) x(pw_samples)];
yfill = [0 50 50 0];
fill(xfill,yfill,'y');
hold off
text(x(pw_samples)/2,25,'Pulse',...
    'HorizontalAlignment','Center','VerticalAlignment','Bottom');
text(x(pw_samples)/2,25,'Width',...
    'HorizontalAlignment','Center','VerticalAlignment','Top');
text(x(1),25,'↖',...

```

```

'HorizontalAlignment','Left','VerticalAlignment','Middle');
text(x(pw_samples),25,'rightarrow',...
'HorizontalAlignment','Right','VerticalAlignment','Middle');

% Plot cross sections in time through the target and the artifact for
% comparison with the analysis (Figure 2.2)
time = (0:pri_samples-1)/fs*1e6;      % time in microseconds
if rise == 0
    figure;
    plot(time,target-max(target));
    hold on
    % - shade in the pulse time
    xfill = [time(1) x(1:pw_samples) time(pw_samples)];
    yfill = [-70 0*artifact(1:pw_samples)-55 -70];
    fill(xfill,yfill,'y');
    plot(time,artifact-max(target),':');
    hold off
    axis([0 max(time) -70 15]);
    % - label the plot
    ix = find(target == max(target));
    ix = ix(1);
    text(time(ix),3,'Target');
    ix = find(artifact == max(artifact));
    ix = ix(1);
    text(time(ix),max(artifact)-max(target)+3,'Artifact');
    xlabel('Time (\muSec)');
    ylabel('Relative Power (dB)');
    text(time(pw_samples)/2,-63,'Pulse',...
        'HorizontalAlignment','Center','VerticalAlignment','Bottom');
    text(time(pw_samples)/2,-63,'Width',...
        'HorizontalAlignment','Center','VerticalAlignment','Top');
    text(time(1),-63,'rightarrow',...
        'HorizontalAlignment','Left','VerticalAlignment','Middle');
    text(time(pw_samples),-63,'rightarrow',...
        'HorizontalAlignment','Right','VerticalAlignment','Middle');
end

% Compute the relative power levels
max_leading = max(artifact(1:pw_samples));
max_trailing = max(artifact(pw_samples+1:pri_samples));
fprintf(1,'The target to leading artifact ratio is %.1f dB.\n',...
    max(target)-max_leading);
fprintf(1,'The target to trailing artifact ratio is %.1f dB.\n',...
    max(target)-max_trailing);

artifact = artifact - max(target);

return;

```

REFERENCES

1. J.L. Eaves and E.K. Reedy (editors), *Principles of Modern Radar*, Chapman and Hall, New York, New York, 1987
2. E. Butkov, *Mathematical Physics*, Addison-Wesley Publishing Company, Reading, Massachusetts, 1968.
3. MATLAB, The Language of Technical Computing, The Math Works, Inc., Natick, Massachusetts, 1996.
4. Digital Signal Processing and Data Acquisition, Pentek 1997 Product Catalog, Pentek, Inc., Upper Saddle River, New Jersey, pp. 83-84.
5. Digital Signal Processing and Data Acquisition, Pentek 1997 Product Catalog, Pentek, Inc., Upper Saddle River, New Jersey, pp. 93-94.
6. Graychip 1012 Product Description, Graychip DSP Chips and Systems, Palo Alto, Ca., 1998
7. G.V. Morris, *Airborne Pulsed Doppler Radar*, Artech House, Norwood, Massachusetts, 1988.

UNCLASSIFIED

-29-

SECURITY CLASSIFICATION OF FORM
(highest classification of Title, Abstract, Keywords)

DOCUMENT CONTROL DATA

(Security classification of title, body of abstract and indexing annotation must be entered when the overall document is classified)

1. ORIGINATOR (the name and address of the organization preparing the document. Organizations for whom the document was prepared, e.g. Establishment sponsoring a contractor's report, or tasking agency, are entered in section 8.) Defence Research Establishment Ottawa 3701 Carling Avenue Ottawa, ON K1A 0Z4		2. SECURITY CLASSIFICATION (overall security classification of the document, including special warning terms if applicable) UNCLASSIFIED
3. TITLE (the complete document title as indicated on the title page. Its classification should be indicated by the appropriate abbreviation (S,C or U) in parentheses after the title.) Mitigation of Transient Doppler Artifacts in Airborne Pulse Doppler Radar (U)		
4. AUTHORS (Last name, first name, middle initial) Hughes, Steven J.		
5. DATE OF PUBLICATION (month and year of publication of document) December 1999	6a. NO. OF PAGES (total containing information. Include Annexes, Appendices, etc.) 39	6b. NO. OF REFS (total cited in document) 7
7. DESCRIPTIVE NOTES (the category of the document, e.g. technical report, technical note or memorandum. If appropriate, enter the type of report, e.g. interim, progress, summary, annual or final. Give the inclusive dates when a specific reporting period is covered.) DREO Technical Report		
8. SPONSORING ACTIVITY (the name of the department project office or laboratory sponsoring the research and development. Include the address.)		
9a. PROJECT OR GRANT NO. (if appropriate, the applicable research and development project or grant number under which the document was written. Please specify whether project or grant) 1410AR/3de21	9b. CONTRACT NO. (if appropriate, the applicable number under which the document was written)	
10a. ORIGINATOR'S DOCUMENT NUMBER (the official document number by which the document is identified by the originating activity. This number must be unique to this document) DREO Technical Report 99-125	10b. OTHER DOCUMENT NOS. (Any other numbers which may be assigned this document either by the originator or by the sponsor)	
11. DOCUMENT AVAILABILITY (any limitations on further dissemination of the document, other than those imposed by security classification) (X) Unlimited distribution () Distribution limited to defence departments and defence contractors; further distribution only as approved () Distribution limited to defence departments and Canadian defence contractors; further distribution only as approved () Distribution limited to government departments and agencies; further distribution only as approved () Distribution limited to defence departments; further distribution only as approved () Other (please specify):		
12. DOCUMENT ANNOUNCEMENT (any limitation to the bibliographic announcement of this document. This will normally correspond to the Document Availability (11). However, where further distribution (beyond the audience specified in 11) is possible, a wider announcement audience may be selected.)		

UNCLASSIFIED

SECURITY CLASSIFICATION OF FORM

DDC03 2/06/87

UNCLASSIFIED

SECURITY CLASSIFICATION OF FORM

13. ABSTRACT (a brief and factual summary of the document. It may also appear elsewhere in the body of the document itself. It is highly desirable that the abstract of classified documents be unclassified. Each paragraph of the abstract shall begin with an indication of the security classification of the information in the paragraph (unless the document itself is unclassified) represented as (S), (C), or (U). It is not necessary to include here abstracts in both official languages unless the text is bilingual).

The Defence Research Establishment Ottawa has developed a Digital Radar Receiver and Data Acquisition System as part of an experimental air-to-air surveillance radar that will be used to demonstrate an air-to-air surveillance capability for the Canadian Forces CP-140 Maritime Patrol Aircraft. The report presents an analysis of the radar return signal expected from a point target, and predicts the existence of transient Doppler artifacts associated with the leading and trailing edges of the radar pulses. A software simulation also produces transient Doppler artifacts, and experimental measurements of a simulated target signal confirm their existence. The potential impact of the artifacts on radar performance is discussed, as are techniques to mitigate their deleterious effects.

14. KEYWORDS, DESCRIPTORS or IDENTIFIERS (technically meaningful terms or short phrases that characterize a document and could be helpful in cataloguing the document. They should be selected so that no security classification is required. Identifiers such as equipment model designation, trade name, military project code name, geographic location may also be included. If possible keywords should be selected from a published thesaurus. e.g. Thesaurus of Engineering and Scientific Terms (TEST) and that thesaurus-identified. If it is not possible to select indexing terms which are Unclassified, the classification of each should be indicated as with the title.)

quadrature demodulation
digital demodulation
pulse doppler radar
coherent radar design

UNCLASSIFIED

SECURITY CLASSIFICATION OF FORM